

Article

Force and Pressure Dependent Asymmetric Workspace Research of a Collaborative Robot and Human

Josef Ponikelský¹, Milan Chalupa² , Vít Černohlávek^{1,*}  and Jan Štěrba¹

¹ Faculty of Mechanical Engineering, University of Jan Evangelista Purkyně in Ustí nad Labem, Pasteurova 1, 40096 Ustí nad Labem, Czech Republic; josefponikelsky@seznam.cz (J.P.); jan.sterba@ujep.cz (J.Š.)

² Faculty of Military Technology, University of Defence in Brno, 66210 Brno, Czech Republic; milan.chalupa@unob.cz

* Correspondence: vit.cernohlavek@ujep.cz

Abstract: This article discusses creating a methodology for the asymmetric measuring of values and processes of collision forces and pressures of the collaborative robot dependent on time. Furthermore, it verifies the usefulness of this methodology in practice by successfully performing the experimental measurement and verifying the possibility of using these results by analysing and stating the collaboration level for a robot of the given type. According to the suggested methodology, the measurement results are a specific output based on real measured data, which can be easily rated and can quickly determine the collaborative level of any robot. Measurements were aimed at determining the values of pressure and force with which the robot acts at certain speeds related to distance from the base. Due to the controlled symmetrical impact of the robot on the measuring device, the transfer of energy from the robot to the human body was guaranteed. In theoretical terms, this article primarily provides the assembly of the theoretical foundation of the collaborative environment between humans and robots, and a comprehensive overview of the possibilities of using the technical specification ISO/TS 15066:2016 when deploying a robot in collaboration with humans in a collaborative environment. This new information is highly valuable for both manufacturers and users of collaborative robots. The presented article analyses the possibilities of measuring collaboration and safety elements in cooperation with a robot. The most significant practical benefit is the presentation of a methodology for measuring robot collaboration and verifying its functionality by conducting experimental measurements of robot collaboration according to this methodology. The measurement was performed on a robot made by Universal Robots, model UR10. The measurement coordinates were stationed in a way to create a spatial measurement model. Boundary coordinates of the spatial model were as follows: [450; 200], [450; 500], [850; 200], and [850; 500]. Collisions were measured at 8 different speeds for each coordinate (20 mms⁻¹, 50 mms⁻¹, 100 mms⁻¹, 200 mms⁻¹, 250 mms⁻¹, 300 mms⁻¹, 350 mms⁻¹, and 400 mms⁻¹) to enable the observation of changes in accordance with speed. The measured values indicate a significant fact: the closer the collision is to the robot's base, the higher the collision forces. An important aspect is that the measured values were only for speeds up to 400 mms⁻¹, which is a very low value for industrial use to meet the desired cycle time. It can be stated with absolute certainty that speed has the greatest impact on collision force values. The speed of the collaborative robot arm can therefore be considered a limiting factor for use in industrial applications with a requirement of a short cycle time. Focusing on the results of the measured values, it can be stated that a new finding is the correct design of robotic movements in relation to possible contact with humans is crucial. The result of the measurement according to the proposed methodology is a specific output of realistically measured data, which can be easily evaluated and the level of collaboration of any robot can be quickly determined. The measured data will also serve as a basis for further processing and preparation of new simulation software. It will be possible to use the intended software for detecting and predetermining the safe asymmetric movements of the collaborative robot already at the stage of production preparations, unlike the method of measuring force and pressure on robots which can be used until the time of implementation into production. In the future, this software may also allow users of collaborative robots to easily and quickly evaluate the robots specified.



Citation: Ponikelský, J.; Chalupa, M.; Černohlávek, V.; Štěrba, J. Force and Pressure Dependent Asymmetric Workspace Research of a Collaborative Robot and Human. *Symmetry* **2024**, *16*, 131.

<https://doi.org/10.3390/sym16010131>

Received: 26 December 2023

Revised: 15 January 2024

Accepted: 17 January 2024

Published: 22 January 2024



Copyright: © 2024 by the authors. Licensee MDPI, Basel, Switzerland. This article is an open access article distributed under the terms and conditions of the Creative Commons Attribution (CC BY) license (<https://creativecommons.org/licenses/by/4.0/>).

Keywords: human–robot interaction robot safety; physical contact

1. Introduction

The combination of technological advancement and a shortage of labour is driving rapid development in robotics. In the case of industrial robots, safety is governed by the safety standard ČSN EN ISO 10218 [1]. In the realm of collaborative robots, legislation is evolving more slowly than the technology itself [2]. Until 2016, it was possible to adhere to a single chapter in ČSN EN ISO 10218 that addressed the possibilities of collaboration between robots and humans; however, the definition was insufficient. Therefore, a technical specification, ISO/TS 15066:2016, was issued specifically for collaborative robots [3,4]. Human–robot collaboration places high demands on safety, as the human shares an asymmetric workspace with the robot without protective fencing. A collaborative robot is only safe up to a certain level [5], which is partly recommended by the new technical specification ISO/TS 15066:2016 [6]. This technical specification defines the maximum safe pressures and forces for each part of the body and for different types of collisions. These values can be seen in Table 1. After ensuring that there are no sharp or pointed objects in the area of application, the following maximum forces and pressures must be observed at any contact points. In the aforementioned specification ISO/TS 15066:2016, there are stated boundaries for values of the marginal forces and pressures, which can happen during a collision between a robot and a human. However, the methodology for measuring these values for any type of collaborative robot is not stated anywhere [7,8]. However, after its compilation, it would be necessary to experimentally validate it, use it to conduct measurements, and thereby confirm its practical usability. Its suitability for practical application in determining the collaboration of robots should be conclusively confirmed by utilizing results and data obtained through the application of this measurement methodology to analyse the collaboration of a specific robot type. This would confirm the appropriateness of complementing and expanding the foundations of robot collaboration analysis, as outlined in the international technical specification ISO/TS 15066:2016 [9,10].

In order to determine force and pressure limits, the Medical Faculty of Johannes Gutenberg University Mainz conducted a research project [8] with the DGUV to create a human pain threshold map in conjunction with the IFA (Institut für Arbeitsschutz der DGUV—Institute for Occupational Safety and Health). The pain threshold map is based on a body model with 15 discrete body regions defined for designing workplaces using collaborative robots. In total, 29 body regions were studied. (see Figure 1). Pain thresholds were determined by pressure algometry. To this end, the IFA has developed a test apparatus using an automatic pressure algometer. The high number of test subjects (approximately 100) allowed us to obtain approximately 9000 analysable pain threshold measurements. The relevant factors affecting the measurements were evaluated by statistical analysis of the measured data [10,11].

The project yielded significant quasi-static force and pressure limits for the human pain threshold. These limits have been incorporated into a technical specification (ISO/TS 15066:2016, supplement to ISO 10218-2) and an informative DGUV publication on the use of collaborative robots [11,12].

Kossman's work [6] focuses on integrating the requirements of ISO ISO/TS 15066:2016 into the systems planning process. Based on the analysis of safety requirements, the influencing variables of collision force and surface pressure occurring in contact between humans and robots are derived. Using a theoretical analysis of the collision mechanics that occur, causal relationships between the influencing variables can be derived. These are investigated experimentally in a series of tests on a test stand.

Table 1. Biomechanical limits according to ISO/TS 15066:2016.

Body Part	Num. Desig. of a Point on the Body Model	Specific Body Region	Quasi-Static Contact		Transient Contact	
			Max. Allowable Pressure ps (N/cm ²)	Max. Allowable Force	Multiplier of Max. Allowable Pressure pT	Multiplier of Max. Allowable Force FT
Skull and forehead	1	Middle of forehead	130	130	Not applicable	Not applicable
	2	Sleep	110		Not applicable	
Face	3	Masticatory muscles	110	65	Not applicable	Not applicable
	4	Neck muscle	140			
Neck	5	Seventh neck vertebra	210	150	2	2
	6	Shoulder joint	160			
Back and shoulders	7	Fifth lumbar vertebra	210	210	2	2
	8	Breast bone	120			
Chest	9	Pectoral muscle	170	140	2	2
	10	Abdominal muscle	140			
Abdomen	11	Pelvic bone	210	180	2	2
	12	Deltoid muscle	190			
Pelvis	13	Humerus	220	150	2	2
	14	Radial bone	190			
Arms and elbow joints	15	Forearm muscle	180	160	2	2
	16	Axillary nerves	180			
Forearm and wrist	17	Pad of index finger D	300	140	2	2
	18	Pad of index finger ND	270			
Hands and fingers	19	Terminal joint of index finger D	280	140	2	2
	20	Terminal joint of index finger ND	220			
Hands and fingers	21	Muscles of the palm	200	140	2	2
	22	Palm D	260			
Hands and fingers	23	Palm ND	260	140	2	2
	24	Back of the hand D	200			
Hands and fingers	25	Back of the hand ND	190	140	2	2
	26	Thigh muscle	250			
Thighs and knees	27	Patella	220	220	2	2
	28	Middle of shin	220			
Lower limbs	29	Calf muscle	210	130	2	2

The work [7] by Švarný focuses on the PFL cooperation regime. It measures the forces exerted by two cooperating collaborative robots (UR10e and KUKA LBR iiwa) on the impact measurement device at different positions in the robot workspace. A 3D collision force map is created with respect to speed, distance from the robot base, and now also height in the workspace. They analyse the behaviour of two collaborative robots, UR10e and KUKA LBR iiwa. The author's measurements show that speed has a large effect on the robot's impact with the obstacle and can lead to impacts of over 446 N, especially near the base. Conversely, if the task is carried out at a distance of 0.8 m and 0.4 m above the robot base, for example, speeds of 0.35 m/s (UR10e) and 0.4 m/s (KUKA LBR iiwa) can be safely controlled while maintaining the prescribed force limit.

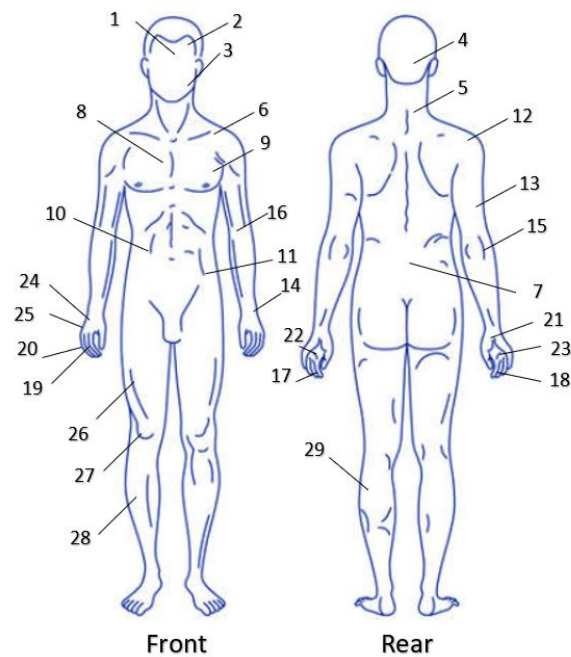


Figure 1. A body model according to ISO/TS 15066:2016 [3] with 29 marked body regions.

2. Design of Measurement Methodology

The aim of the experiment is to analyse the movements of the collaborative robot and its subsequent collision with a measuring fixture representing a human body part. The measured values will be compared with the limits given in ISO TS 15066:2016.

In order to comply with the force and pressure limit values according to ISO/TS 15066:2016, it is necessary to measure these values during the given movements of the collaborative robot [13,14]. For this purpose, a measuring device is used which resembles the human body in its mechanical properties [15]. Testing the permissible stress level according to existing standards requires the measurement, analysis, and evaluation of the maximum collision force and the local maximum pressure occurring in the plane of collision [16].

The CoboSafe force and pressure measurement system (see Figure 2) meets all the requirements necessary to verify and comply with the limit values and is adapted to each application area [17]. Depending on the requirement and the target, up to nine force transducers with different spring constants can be assembled. The combination of spring constants with one of the damping elements allows the biomechanical properties to be configured according to ISO/TS 15066:2016.

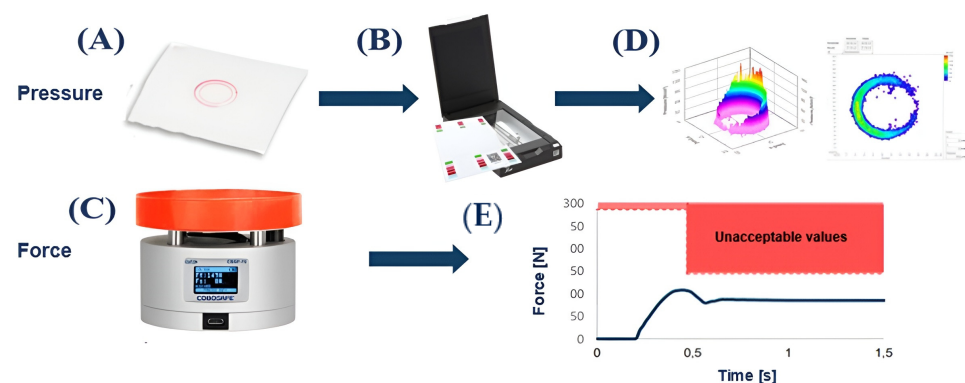


Figure 2. The CoboSafe measuring instrument system, which consists of pressure films (A), scanner (B), measuring piston (C), and software for evaluating forces and pressures (D,E).

The main part of the sensor [18] is a piezoelectric force transducer with a linearly guided measuring mechanism, which guarantees optimum accuracy and reproducibility of the measurement. The meter is equipped with integrated electronics for evaluation and storage of measured values [19].

The CoboSafe-Scan kit is based on Fujifilm Prescale measuring films. It records pressure distribution and maximum pressure. The films respond to pressure and show the pressure distribution. The pressure force is determined by the intensity of the colouration of the pressure measurement films. Using the scanner and calibration sheet, the pressure image is imported into the CoboSafe-Vision software (version number 1.2.10.611) and the data is automatically evaluated. The imported pressure film is converted to pressure values and the result displays the pressure image and the maximum pressure [20].

A collision map (Figure 3) was created for the experiment, which shows the collision coordinates relative to the robot base [21]. The collision map was designed to verify the force and pressure data as specified in ISO/TS 15066:2016 [22]. In each coordinate, the robot was programmed to strike the CoboSafe CBSF-75 measuring fixture (Figure 2) The robot in that coordinate was always tested for speeds according to Table 2. Pressure measurements were always taken at the extreme positions of the collision map for speeds v_1 , v_4 and v_8 .

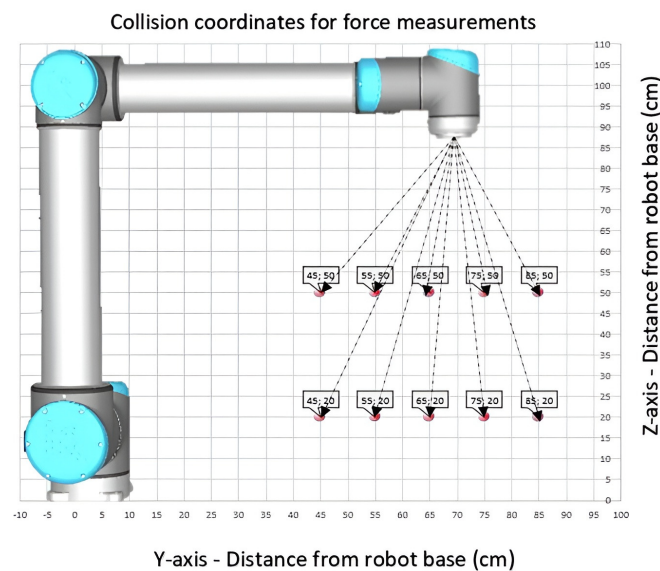


Figure 3. Force measurement coordinates, UR10 robot.

Table 2. Specified measurement values.

Value Name	Value Designation	Value	Unit
Horizontal coordinates of distance of force F_x from robot base	Y_x	450–850	mm
Vertical coordinates of the distance of the force F_x from the robot base	Z_x	200–500	mm
Collision speed of the robot arm	v_1	20	mms^{-1}
Collision speed of the robot arm	v_2	50	mms^{-1}
Collision speed of the robot arm	v_3	100	mms^{-1}
Collision speed of the robot arm	v_4	200	mms^{-1}
Collision speed of the robot arm	v_5	250	mms^{-1}
Collision speed of the robot arm	v_6	300	mms^{-1}
Collision speed of the robot arm	v_7	350	mms^{-1}
Collision speed of the robot arm	v_8	400	mms^{-1}

The coordinates of the collision and the coordinates of the target point of the robot are intentionally different so that the measurement is not affected by the collision occurring in the same coordinate as the programmed robot. This difference resulted in an unexpected collision of the robot with the measuring fixture. The coordinates of the robot contact with the measuring fixture for the UR10 robot are given in the force measurement collision map in Figure 3.

A structure (see Figure 4) consisting of aluminium profiles, interconnecting parts, linear guides, and metering was assembled for fixing the measuring fixture. The linear guide was used to position the trolley on which the CBSF-75 fixture was mounted and the trolley was positioned along the Y-axis to the given coordinates [450, 550, 650, 750, and 850]. The trolley had an integrated locking mechanism to fix the position during measurement. After measuring all the specified values from 450 mm to 850 mm in the Y-axis, the fixture and measuring device were moved to a height of 500 mm in the Z-axis. The measurement process was repeated again by moving the fixture in the Y-axis from 450 mm to 850 mm [23].

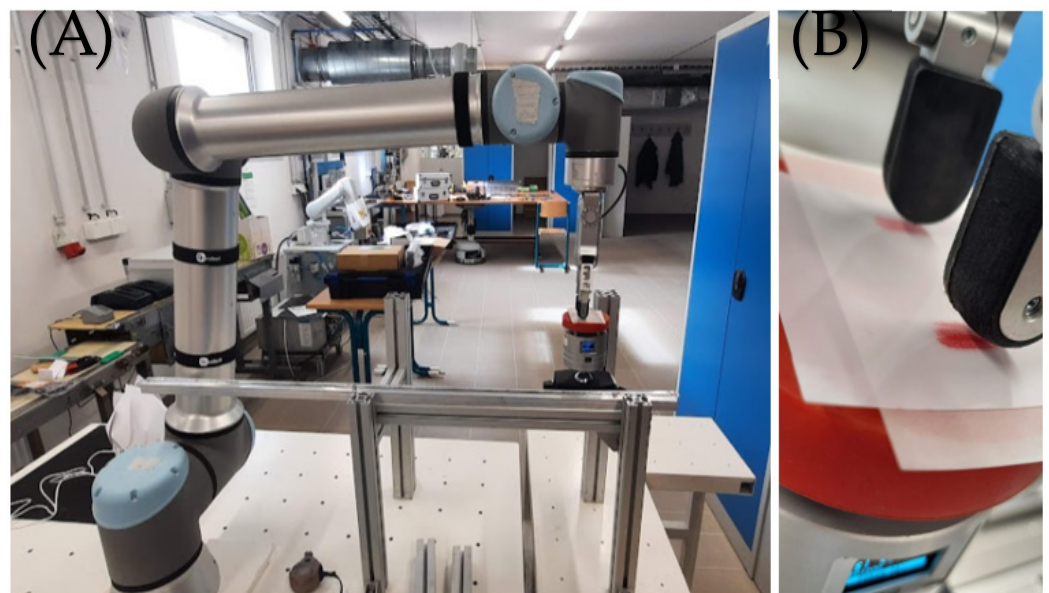


Figure 4. (A) Demonstration of a structure with a measuring fixture, (B) OnRobot RG2 gripper on the UR10 robot and measuring pressure films after collision.

Coordinates for the starting point for robot UR10 are shown in Table 3, together with coordinates of the target point, which was input into the robot's program as target point for given linear movement. The coordinates of the collision and the coordinates of the target point of the robot are intentionally different so that the measurement is not affected by the collision occurring in the same coordinate as the programmed robot. This difference resulted in an unexpected collision of the robot with the measuring fixture $v_1 = 20 \text{ mms}^{-1}$, $v_2 = 50 \text{ mms}^{-1}$, $v_3 = 100 \text{ mms}^{-1}$, $v_4 = 200 \text{ mms}^{-1}$, $v_5 = 250 \text{ mms}^{-1}$, $v_6 = 300 \text{ mms}^{-1}$, $v_7 = 350 \text{ mms}^{-1}$, and $v_8 = 400 \text{ mms}^{-1}$. Next are shown values for coordinates of the collision, which correspond to the coordinates of the upper position of the measuring jig in the given position. The robot movements were programmed in jogging mode and, at the time of the collision, there was a constant speed between points [24]. This method was chosen primarily due to the predictability of movements relative to the measuring fixture.

Table 3. Coordinates of collision points and UR robot’s target points.

	Coordinates of Robot’s Starting Point:			Coordinates of Robot’s Target Point:			Coordinates of the Collision between the Robot and the Jig		
	X	Y	Z	X	Y	Z	X	Y	Z
Bottom position:	0	720	780	0	450	140	0	450	200
	0	720	780	0	550	140	0	550	200
	0	720	780	0	650	140	0	650	200
	0	720	780	0	750	140	0	750	200
	0	720	780	0	850	140	0	850	200
Upper position:	0	720	780	0	450	440	0	450	500
	0	720	780	0	550	440	0	550	500
	0	720	780	0	650	440	0	650	500
	0	720	780	0	750	440	0	750	500
	0	720	780	0	850	440	0	850	500

3. Measurements Performed

A total of 80 measurements were performed to obtain the collision force values for the UR10 robot. The measured transient and quasi-static collision forces for the UR10 robot are given in Table 3. In addition to the measured values of quasi-static forces at low speed v_1 , for almost all coordinates except for the [450; 500] and [550; 500] coordinates and the speed v_3 of the [650; 500] coordinate, the forces were evaluated as transient, for example, the measured value of 133/130 N for the collision coordinate [450; 200], where 133 N is the transient force and the value of 130 N is the quasi-static force that acted for more than 0.5 s.

In Table 4, the measured values that correspond to the maximum allowable force in [N] for transient and quasi-static contact were marked in green and the forces that do not correspond to the maximum allowable forces according to ISO/TS 15066:2016 were marked in red. In our case, the limits for transient contact were $F_t = 280$ N and for quasi-static contact $F_s = 140$ N. The CBSF measuring fixture has a measurement tolerance of ± 15 N. The robot’s speed at the time of the collision is equal to the speed of the robot arm listed in the table under the designations $v_1, v_2, v_3, v_4, v_5, v_6, v_7$, and v_8 . All measured values during the measurement showed no error. The measurement system was assembled in a way that, upon impact, the value was measured and subsequently recorded in the table.

Table 4. Measured data—UR10, collision force.

Force Measurement Ft/Fs [N]				Universal Robots UR-10 Robot Arm Speed							
Meas. No.	Coordinates of Distance of Fixture from Robot Base [Y;Z]			$v_1 = 20$ mms ⁻¹	$v_2 = 50$ mms ⁻¹	$v_3 = 100$ mms ⁻¹	$v_4 = 200$ mms ⁻¹	$v_5 = 250$ mms ⁻¹	$v_6 = 300$ mms ⁻¹	$v_7 = 350$ mms ⁻¹	$v_8 = 400$ mms ⁻¹
1	až	8	450; 200	133/130	153	179	231	244	286	315	376
9	až	16	450; 500	85	88	94	104	115	138	161	163
17	až	24	550; 200	128/125	143	163	219	269	302	333	369
25	až	32	550; 500	95	101	119	132	154	177	207	234
33	až	40	650; 200	91/84	109	127	201	218	219	257	283
41	až	48	650; 500	98/84	167/92	124	123	142	172	206	236
49	až	56	750; 200	102/96	114	141	200	236	260	296	350
57	až	64	750; 500	116/115	120	128	146	152	175	207	244
65	až	72	850; 200	125/117	139	152	173	250	288	322	361
73	až	80	850; 500	110/110	118	121	144	164	202	233	261
Limit value according to ISO TS 15066:						Transient 280 N/Quasi-static 140 N (15 N tolerance)					

Figure 5 was created based on the values in Table 3. The red horizontal line F_t in the graph shows the maximum allowable force for transient contact, which for the hand area is 280 N. The purple horizontal line F_s shows the maximum allowable force for quasi-static contact with a value of 140 N. Values above these lines are not permissible for quasi-static or transient collision forces according to ISO/TS 15066:2016:2016. It can also be seen from the graph that the forces measured when the fixture is placed further away from the base in the Z-axis direction (i.e., at a height of 500 mm from the robot base) are smaller than the values for a fixture placed lower down (i.e., at a height of 200 mm from the robot base). The graph also shows the dependence of the robot arm speed on the collision force. In the following, the data measured in the coordinates [450; 200] and [450; 500] for the speed 20 mms^{-1} , 200 mms^{-1} , and 400 mms^{-1} will be discussed.

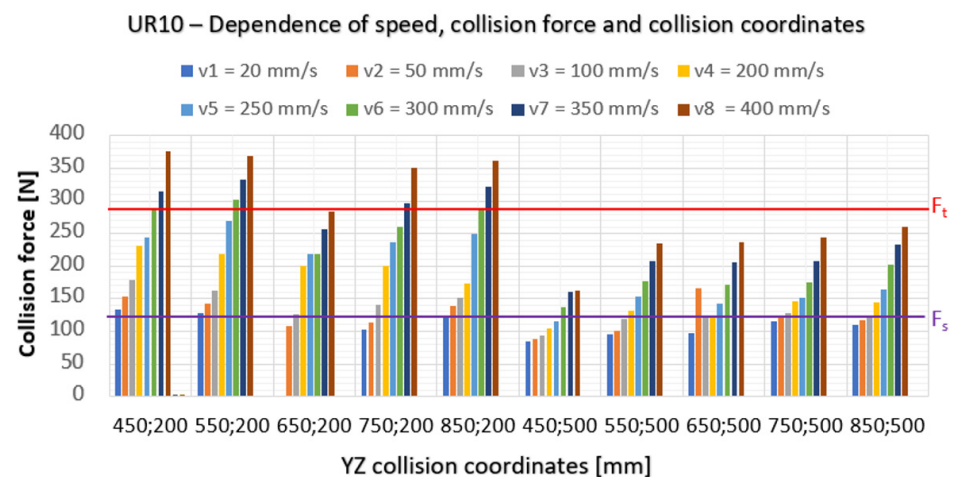


Figure 5. UR10 Dependence of collision force and collision coordinates.

4. Evaluation of Measurements and Discussion

4.1. UR—Measurement in Coordinate [450; 200], Speed $v = 20 \text{ mms}^{-1}$

In Figure 6, it can be observed that the motion is quasi-static, as the force value was recorded for more than 0.5 s, approximately the time corresponds to 0.7 s. The measured force for the quasi-static collision was measured to be 130 N, the largest collision value was for the transient motion 133 N. Both values correspond to the maximum allowable forces. On the pressure graph, it can be seen that the measured pressure is greater than 300 N/cm^2 and therefore does not correspond to the permissible pressure values for quasi-static contact.

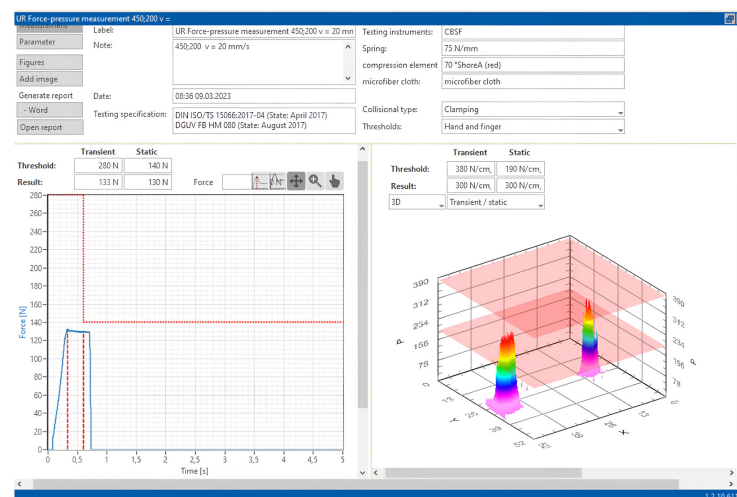


Figure 6. Measured data in CoboSafe for coordinate [450; 200], speed 20 mms^{-1} .

The position of the joints of the UR10 robot in the collision with the measuring fixture in the [450; 200] coordinate can be observed in Figure 7.



Figure 7. Position of UR arm joints in collision in coordinate [450; 200].

4.2. UR—Measurement in Coordinate [450; 200], Speed $v = 200 \text{ mm s}^{-1}$

In Figure 8, it can be observed, compared to the previous measurement at lower speed, that it is no longer a quasi-static collision but a transient collision at 200 mm s^{-1} because the applied force was shorter than 0.5 s. In this case, the force was applied for approximately 0.25 s. The measured force of 231 N is within the range for a transient collision. The measured pressure is greater than 300 N/cm^2 , probably even greater than the permissible value of 380 N/cm^2 . Due to the LWW film used, we cannot determine the maximum pressure value. LW film would have to be used here for values of $250\text{--}500 \text{ N/cm}^2$. However, such high values were not considered when making the purchase and therefore only LWW film was purchased for values up to 250 N/cm^2 . The measured pressure can be estimated with respect to the measured values and the area on which it acts to a maximum value of 400 N/cm^2 .

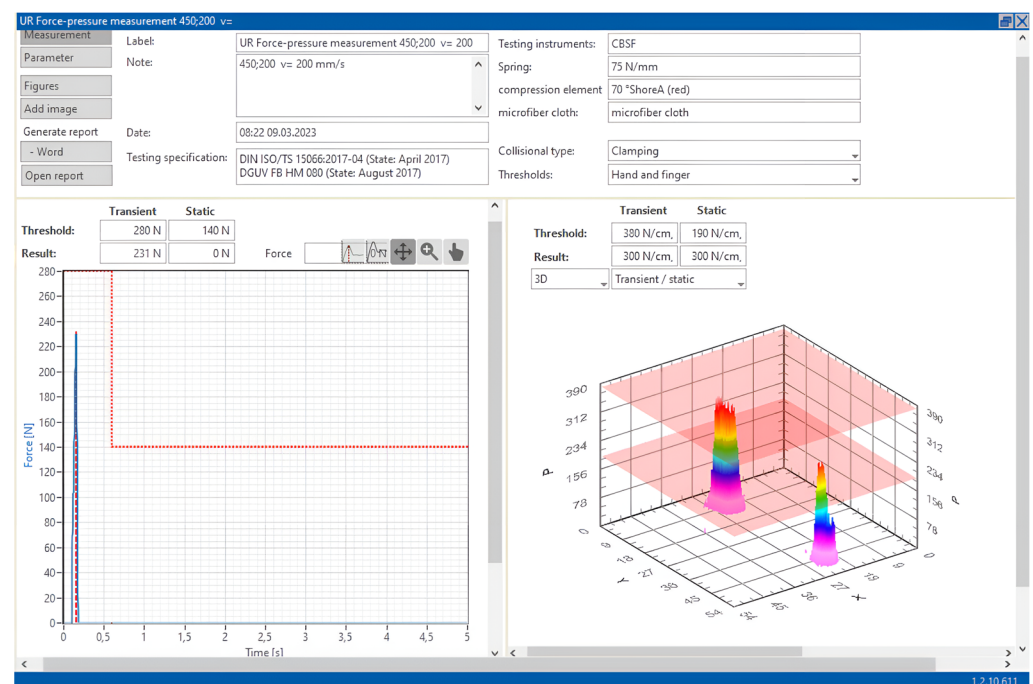


Figure 8. Measured data in CoboSafe for coordinate [450; 200], speed $v = 200 \text{ mm s}^{-1}$.

4.3. UR—Measurement in Coordinate [450; 200], Speed $v = 400 \text{ mms}^{-1}$

In Figure 9, it can be observed for the speed $v = 400 \text{ mms}^{-1}$ that the already measured force of 370 N does not correspond to the values of the permissible force for transient motion. The measured pressure can be estimated at 450 N/cm^2 out of a possible allowable pressure of 380 N/cm^2 .

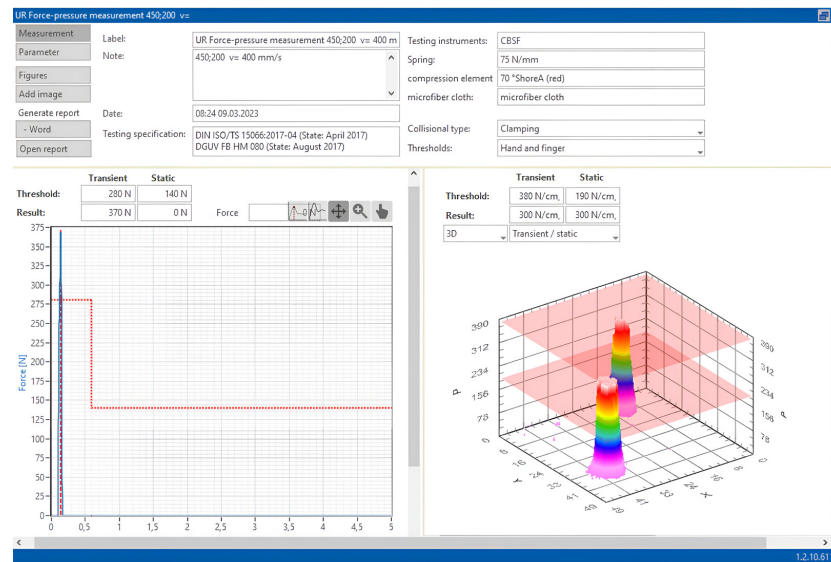


Figure 9. Measured data in CoboSafe for coordinate [450; 200], speed $v = 400 \text{ mms}^{-1}$.

4.4. UR—Measurement in Coordinate [450; 500], Speed $v = 20 \text{ mms}^{-1}$

Figure 10 shows the values from the measurements for the coordinate [450; 500] and therefore this is the upper position of the measurements. The measured force is 85 N and was applied for approximately 0.6 s and this collision can be considered as quasi-static. The measured pressure was greater than 190 N/cm^2 and does not correspond to the allowable pressure for a quasi-static collision. A larger area can be observed on the measured area of applied pressure than for low-position measurements. This can be attributed to the trajectory of the motion the robot was performing just before the collision.

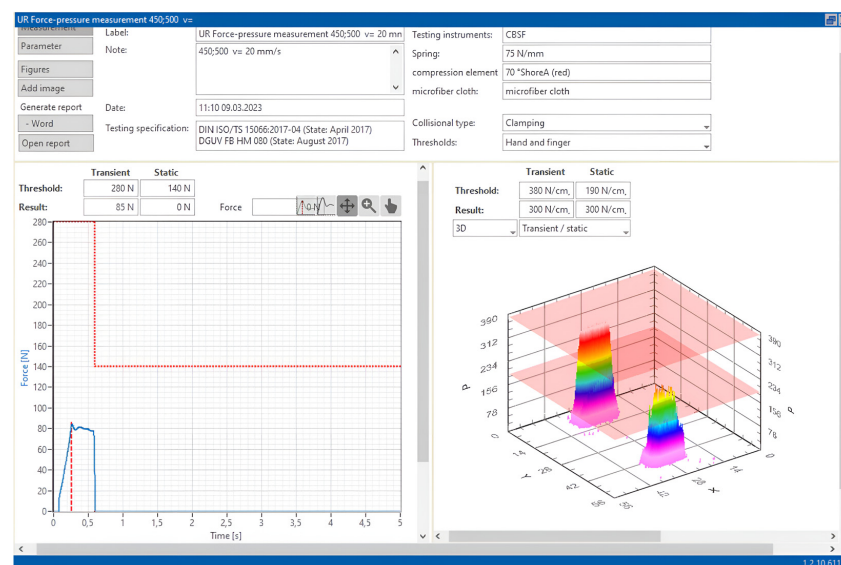


Figure 10. Measured data in CoboSafe for coordinate [450; 500], speed $v = 20 \text{ mms}^{-1}$.

The position of the individual joints in the collision between the robot and the measuring fixture in the [450; 500] coordinate is shown in Figure 11.



Figure 11. Position of the UR10 arm joints in a collision in coordinate [450; 500].

4.5. UR—Measurement in Coordinate [450; 500], Speed $v = 200 \text{ mms}^{-1}$

In Figure 12, the measured force can be seen with a value of 105 N, which corresponds to the allowed value of the transient contact force due to the applied time of 0.2 s. The measured pressure was greater than 300 N/cm^2 and does not correspond to the allowable pressure for a quasi-static collision. A larger area can be observed on the measured area of applied pressure than that for low-position measurements. This can be attributed to the trajectory of the motion the robot was performing just before the collision.

4.6. UR—Measurement in Coordinate [450; 500], Speed $v = 400 \text{ mms}^{-1}$

The measured force for speed $v = 400 \text{ mms}^{-1}$ for the collision coordinate in the upper position closer to the base is shown in Figure 13 and its value is 164 N. The force corresponds to the allowed range for transient motion. The pressure was measured above 300 N/cm^2 and is estimated to be approximately 500 N/cm^2 , which does not correspond to the permissible values.

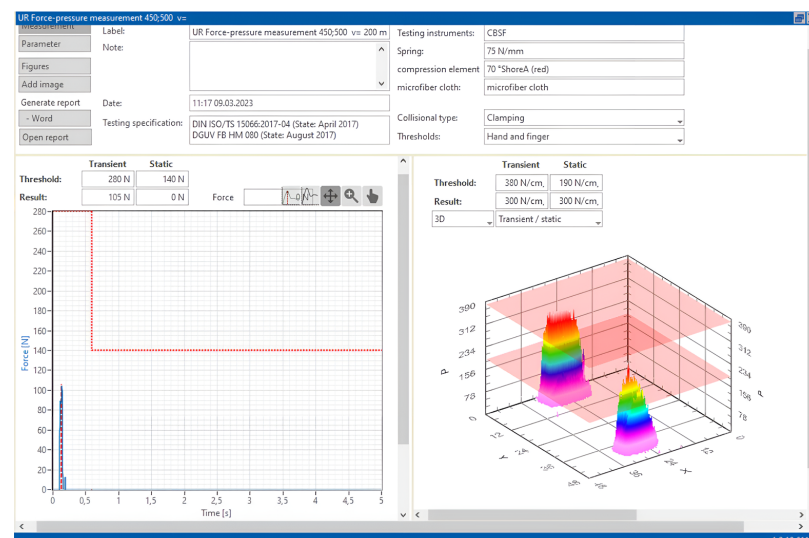


Figure 12. Measured data in CoboSafe for coordinate [450; 500], speed $v = 200 \text{ mms}^{-1}$.

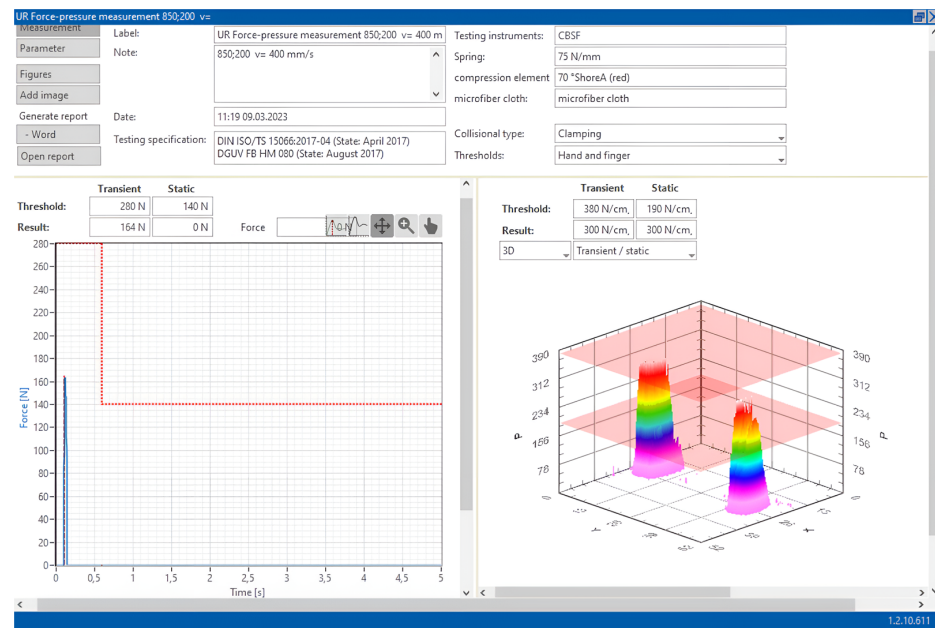


Figure 13. Measured data in CoboSafe for coordinate [450; 500], speed $v = 400 \text{ mms}^{-1}$.

5. Conclusions

On a theoretical level, this research provides a basic overview of the definition and measurement of an asymmetric collaborative space. The biggest benefit in the theoretical sphere seems to be creating a theoretical basis of the measurement of a collaborative environment between a human and a robot.

First, a set of monitored parameters for safe collaboration was assembled: force, pressure, distance, and speed parameters. Afterwards, a methodology proposal for measuring input data from a simulation of robotic work in a collaborative environment was made. The next partially fulfilled step was verifying the functionality of the proposed methodology by performing an experimental measurement according to this proposed methodology.

From the measured values followed critical information: that the closer a collision is to the base of the robot, the higher are the collision forces. As we can see in Table 4, the coordinate of the distance of the fixture from the robot base [450; 200] was already measured as unsatisfactory from a speed of 300 mms^{-1} , i.e., over a value of 280 N, and the same was the case for the collision coordinate [550; 200]. For the coordinates of the distance of the fixture from the base of the robot [750; 200] and [850; 200], overlimit forces were measured from a speed of 350 mms^{-1} . This speed was determined on the basis of similar testing [7]. It can be observed that at higher speeds above 400 mms^{-1} , the values would already exceed the permissible limit. It can be said with absolute certainty that speed has the biggest impact on the value of collision force.

In the evaluation, only the collision force was evaluated, due to all measured high-pressure values that exceeded the permissible limit for TR = transient collision 380 N/cm and for QS = quasi-static collision 190 N/cm . The pressure measurement was affected by the choice of gripper and the fingers used for the test. In order to also be able to evaluate the test for forces, we consider the pressures to be unimportant, because the object of the test is primarily the robot and not the gripper. For accurate pressure measurements, tests need to be carried out on LW-type films, which can record higher pressures of up to 500 N/cm^2 .

Of the 80 measured forces of the UR10 collaborative robot listed in Table 3, a total of 70 collisions were in accordance with ISO/TS 15066:2016. It can be concluded that for speeds up to 250 mms^{-1} , all tests performed were in accordance with the maximum permissible value of the collision force for both quasi-static and transient contact. For speeds above 250 mms^{-1} , only the values measured in the lower position of the collision coordinate were critical, except for the [650; 200] coordinate where the measured value

was consistent even at a measured speed of 400 mms^{-1} . If we were to further increase the speeds by another 100 mms^{-1} , it can be assumed that the coordinates that were measured in accordance with the maximum allowable value would already show a value above the maximum allowable value.

Based on this and other experimental measurements focusing on the topic of robot path trajectory and safety, in the second article, software will be designed to calculate the safe movements of robots with regard to cooperation with humans.

Author Contributions: Conceptualization, J.P. and M.C.; methodology, M.C.; validation, V.Č., J.Š., J.P. and M.C.; formal analysis, J.P. and J.Š.; investigation, V.Č. and M.C.; data curation, V.Č. and M.C.; writing—original draft preparation, J.P. and J.Š.; writing—review and editing, V.Č. All authors have read and agreed to the published version of the manuscript.

Funding: This research received no external funding.

Institutional Review Board Statement: The study was conducted in accordance with the Declaration of Helsinki and approved by the Institutional Review Board (or Ethics Committee) of the Ethics Committee of Faculty of Mechanical Engineering Jan Evangelista Purkyně University in Usti nad Labem.

Informed Consent Statement: Informed consent was obtained from all subjects involved in the study.

Data Availability Statement: Data are contained within the article.

Conflicts of Interest: The authors declare no conflicts of interest.

References

1. ČSN EN ISO 10218-2; Roboty a Robotická Zařízení—Požadavky na Bezpečnost Průmyslových Robotů: Část 2: Systémy Robotů a Integrace. Český Normalizační Institut: Prague, Czech Republic, 2011.
2. Javerník, A.; Kovič, K.; Palčič, I.; Ojsteršek, R. Audio-Visual Effects of a Collaborative Robot on Worker Efficiency. *Symmetry* **2023**, *15*, 1907. [CrossRef]
3. ISO/TS 15066; Robots and Robotic Devices—Collaborative Robots. International Organization for Standardization: Geneva, Switzerland, 2016.
4. Matthias, B.; Reisinger, T. Example Application of ISO/TS 15066 to a Collaborative Assembly Scenario. In Proceedings of the ISR 2016 47st International Symposium on Robotics, Munich, Germany, 21–22 June 2016; pp. 1–5.
5. Rodday, V.; Geißler, B.; Letzel, S.; Muttray, A.; Huelke, M.; Ottersbach, H.J. *Druckschmerzschwellen bei Druckreizen*, 51. Jahrestagung der Deutschen Gesellschaft für Arbeitsmedizin und Umweltmedizin (DGAUM); Triebig, G., Ed.; Deutsche Gesellschaft für Arbeitsmedizin und Umweltmedizin: Aachen, Germany; 9–12 März 2011, pp. 828–829. ISBN 978-3-9811784-5-6.
6. Kossman, M. Sicherheit in der Mensch-Roboter-Interaktion durch Einen Biofidelen Bewertungsansatz. Ph.D. Thesis, Technische Universität München, München, Germany, 2019.
7. Švarný, P. *3D Collision-Force-Map for Safe Human-Robot Collaboration*; ČVUT: Prague, Czech Republic, 2020.
8. Behrens, R.; Zimmermann, J. Determination of Biomechanical Corridors for the Evaluation of Mechanical Hazards and Estimation of Stiffness Parameters for Future Measurement Devices—Final Report on the Research Project of Fraunhofer IFF and IFA. 2021. Available online: https://www.dguv.de/medien/ifa/en/fac/kollaborierende_roboter/ifa-skl_final_report.pdf (accessed on 3 November 2021).
9. Suszyński, M.; Peta, K.; Černošlák, V.; Svoboda, M. Mechanical Assembly Sequence Determination Using Artificial Neural Networks Based on Selected DFA Rating Factors. *Symmetry* **2022**, *14*, 1013. [CrossRef]
10. Suszynski, M.; Wojciechowski, J.; Zurek, J. No Clamp Robotic Assembly with Use of Point Cloud Data from Low-Cost Triangulation Scanner. *Teh. Vjesn.* **2018**, *25*, 904–909. [CrossRef]
11. Klimenda, F.; Cizek, R.; Suszynski, M. Measurement of a Vibration on a Robotic Vehicle. *Sensors* **2022**, *22*, 8649. [CrossRef] [PubMed]
12. Ponikelsky, J.; Cernohlavek, V.; Sterba, J.; Houska, P. Research of Robots in Cooperative Mode in Human Body Part Detection. *Manuf. Technol.* **2023**, *23*, 99–109. [CrossRef]
13. Mathavan Jeyabalan, P.K.; Nehrujee, A.; Elias, S.; Magesh Kumar, M.; Sujatha, S.; Balasubramanian, S. Design and Characterization of a Self-Aligning End-Effector Robot for Single-Joint Arm Movement Rehabilitation. *Robotics* **2023**, *12*, 149. [CrossRef]
14. Zhang, X.; Yang, F.; Jin, Q.; Lou, P.; Hu, J. Path Planning Algorithm for Dual-Arm Robot Based on Depth Deterministic Gradient Strategy Algorithm. *Mathematics* **2023**, *11*, 4392. [CrossRef]
15. Pástor, M.; Hagara, M.; Gašpár, Š.; Sapieta, M. Design and Implementation of a Low-Cost Torque Sensor for Manipulators. *Appl. Sci.* **2023**, *13*, 9406. [CrossRef]
16. Suszyński, M.; Peta, K. Assembly Sequence Planning Using Artificial Neural Networks for Mechanical Parts Based on Selected Criteria. *Appl. Sci.* **2021**, *11*, 10414. [CrossRef]

17. Klimenda, F.; Sterba, J.; Cernohlavek, V.; Ponikelsky, J.; Maran, P. Draft of robotic workstation for laser engraving. *Manuf. Technol.* **2021**, *21*, 357–363. [[CrossRef](#)]
18. Batista, J.G.; Ramalho, G.L.B.; Torres, M.A.; Oliveira, A.L.; Ferreira, D.S. Collision Avoidance for a Selective Compliance Assembly Robot Arm Manipulator Using Topological Path Planning. *Appl. Sci.* **2023**, *13*, 11642. [[CrossRef](#)]
19. Carriero, G.; Calzone, N.; Sileo, M.; Pierri, F.; Caccavale, F.; Mozzillo, R. Human-Robot Collaboration: An Augmented Reality Toolkit for Bi-Directional Interaction. *Appl. Sci.* **2023**, *13*, 11295. [[CrossRef](#)]
20. Herbster, S.; Behrens, R.; Elkmann, N. Modeling the Contact Force in Constrained Human-Robot Collisions. *Machines* **2023**, *11*, 955. [[CrossRef](#)]
21. Yan, Y.; Su, H.; Jia, Y. Modeling and Analysis of Human Comfort in Human-Robot Collaboration. *Biomimetics* **2023**, *8*, 464. [[CrossRef](#)] [[PubMed](#)]
22. Cernohlavek, V.; Klimenda, F.; Houska, P.; Suszyński, M. Vibration Measurements on a Six-Axis Collaborative Robotic Arm—Part I. *Sensors* **2023**, *23*, 1629. [[CrossRef](#)] [[PubMed](#)]
23. Toledano-García, A.A.; Pérez-Cabrera, H.R.; Ortega-Cabrera, D.; Navarro-Durán, D.; Pérez-Hernández, E.M. Trajectory Generator System for a UR5 Collaborative Robot in 2D and 3D Surfaces. *Machines* **2023**, *11*, 916. [[CrossRef](#)]
24. Anatoliotakis, N.; Paraskevopoulos, G.; Michalakis, G.; Michalellis, I.; Zacharaki, E.I.; Koustoumpardis, P.; Moustakas, K. Dynamic Human-Robot Collision Risk Based on Octree Representation. *Machines* **2023**, *11*, 793. [[CrossRef](#)]

Disclaimer/Publisher’s Note: The statements, opinions and data contained in all publications are solely those of the individual author(s) and contributor(s) and not of MDPI and/or the editor(s). MDPI and/or the editor(s) disclaim responsibility for any injury to people or property resulting from any ideas, methods, instructions or products referred to in the content.